Manganese Complexes as Drying Catalysts for Alkyd Paints

Gorkum, R. van

3

[Mn(acac)$_3$] as a drying catalyst for alkyd paints.†

Abstract

In this Chapter a study is described of the autoxidation and oligomerisation of the model compound ethyl linoleate (EL), catalysed by [Mn(III)(acac)$_3$] and its combination with bipyridine (bpy). The results are compared with the results for the autoxidation of EL catalysed by the commercial paint driers Co(II) 2-ethylhexanoate (Co-EH) and Mn(II) 2-ethylhexanoate (Mn-EH). The activity of [Mn(III)(acac)$_3$] and [Mn(III)(acac)$_3$]/bpy as driers in real alkyd paint mixtures has been also investigated. The autoxidation of EL was studied through time-resolved Raman spectroscopy, time-resolved Fourier transform infrared spectroscopy, oxygen uptake measurements, and peroxide amount determination. To follow the oligomerisation of EL in time, size exclusion chromatography was used. Head-space GC-MS measurements were performed to determine the amounts of hexanal and pentanal that were formed as volatile byproducts during the autoxidation of EL. The autoxidation rates of EL in the presence of Co-EH and [Mn(acac)$_3$]/bpy were found to be similar, while the reaction rate in the presence of [Mn(acac)$_3$] was slower. The extent of EL oligomerisation was much higher for [Mn(acac)$_3$] compared to the other catalysts. Different mechanisms are proposed for the mode of action for each of the catalysts: Co-EH is primarily a hydroperoxide decomposition catalyst, as is [Mn(acac)$_3$], only the latter one is less active. The [Mn(acac)$_3$]/bpy combination most likely forms the very reactive complexes [Mn(III)(acac)$_2$(bpy)]$^+$ and [Mn(II)(acac)$_2$(bpy)], which are responsible for a very high autoxidation rate, but also for significant degradation of the formed polymer network via β-scission reactions, due to the promotion of alkoxy radical formation.

†Parts of this chapter have been published: R. van Gorkum, E. Bouwman, J. Reedijk, *Inorganic Chemistry*, **2004**, *43*, 2456; R. van Gorkum, E. Bouwman, J. Reedijk *patent EP1382648*, **2004**; Z. O. Oyman, W. Ming, R. van der Linde, R. van Gorkum, E. Bouwman, *Polymer*, **2005**, in press.

3.1 Introduction

Currently, cobalt carboxylates (e.g. cobalt(II) 2-ethylhexanoate, Co-EH) are the most effective, commercially available catalysts for the oxidative drying of alkyd paints (see also Chapter 1).[1] Nevertheless, cobalt compounds are suspected to be *carcinogenic* to tissues and lungs.[2, 3] Due to this fact, it is essential to replace the cobalt complexes used in paint systems with environmentally friendlier alternatives.

The commercially available manganese-based drying catalysts for alkyd paints are manganese carboxylates. Their catalytic activity is, however, much lower than that of cobalt carboxylates. As a consequence, alkyd-based paints containing Mn carboxylates usually suffer from slow drying that leads to undesirable final film properties.[1]

In the course of experiments to develop new drying catalysts based on manganese complexes it was found that [Mn(acac)$_3$] is an excellent autoxidation catalyst for ethyl linoleate (EL), and the addition of bipyridine (bpy) significantly enhances the autoxidation rate. In this Chapter, the catalytic activity of [Mn(acac)$_3$] and its combination with bpy for the autoxidation and oligomerisation of EL was examined using various techniques. The results are discussed in comparison with the catalytic activities of the commercial paint driers cobalt(II) 2-ethylhexanoate (Co-EH) and manganese(II) 2-ethylhexanoate (Mn-EH) that were also determined. A mechanism for the observed high autoxidation rate of the system [Mn(acac)$_3$]/bpy is proposed. Finally, the results are presented of the use of [Mn(acac)$_3$] and [Mn(acac)$_3$]/bpy as driers in real alkyd paint.

3.2 Results

3.2.1 The rate of autoxidation determined by FTIR measurements

The rate of the consumption of EL can be monitored by plotting the natural logarithm of the percentage decrease of the peak integral of the 3010 cm^{-1} peak in the FT-IR spectrum (see Chapter 2, Section 2.2.2). The FTIR plots are depicted in Figure 3.1 and the autoxidation rates and induction times of Mn-EH, Co-EH, [Mn(acac)$_3$], [Mn(acac)$_3$]/bpy and [Mn(acac)$_2$(bpy)] are listed in Table 3.1. Large variations in induction times are observed when unpurified EL is used as the substrate. Unpurified EL

Table 3.1: Oxidation rates and induction times for the oxidation of EL[a]

	Induction time (minutes)	Rate constant k (10^{-3}min^{-1})
Co-EH	0	3
Mn-EH	>700	2
[Mn^{III}(acac)$_3$]	<100	1
[Mn^{III}(acac)$_3$] + 1 eq. Bpy	30	4
[Mn^{III}(acac)$_3$] + 2 eq. Bpy	50	4
[Mn^{III}(acac)$_3$] + 3 eq. Bpy	45	5
[Mn^{II}(acac)$_2$(bpy)]	430	2

[a]EL was purified by eluting over Al_2O_3 before use. No peroxides could be detected in purified EL. Molar ratio catalyst/EL = 1/400, reaction in neat EL at room temperature. Due to the radical nature of the reactions the average experimental error is about 20%.

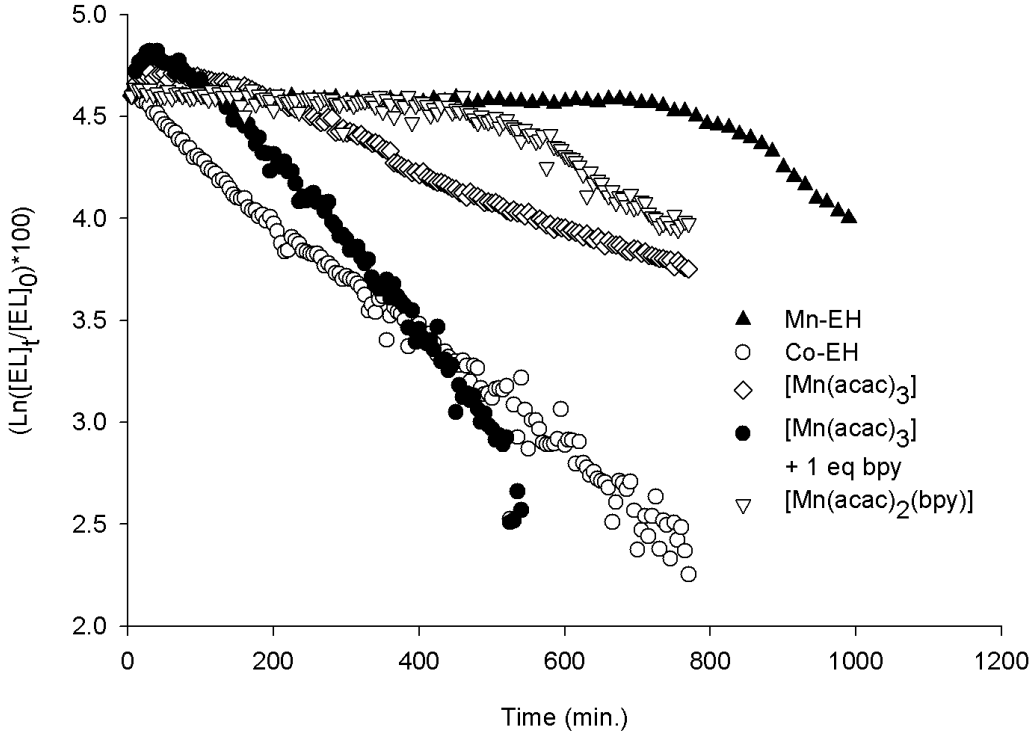

Figure 3.1: Time-dependent integral plots of the 3010 cm^{-1} IR peak of purified EL, reaction with different autoxidation catalysts.

contains hydroperoxides in varying amounts, due to slow air oxidation during storage. The presence of hydroperoxides directly influences the reaction rate and induction time. When *purified* EL is used (all peroxides removed), the induction time for the commercially used manganese catalyst Mn-EH increases from 400 to over 700 minutes. Short induction times (varying between 0–100 minutes) are observed, however, when manganese(III) acetylacetonate is used as an oxidation catalyst. The higher oxidation activity (activity meaning the effectiveness with which EL is consumed in a certain amount of time) for [Mn(acac)$_3$] compared to that of Mn-EH can be attributed mostly to the large induction time for Mn-EH. When the EL oxidation rate for [Mn(acac)$_3$] is compared with the rates for Mn-EH and Co-EH, it is clear that although [Mn(acac)$_3$] shows a slightly lower rate than Co-EH, its overall activity is far superior to that of Mn-EH. Addition of one equivalent of bipyridine to a reaction mixture of [Mn(acac)$_3$] and EL increases the rate of oxidation of EL significantly, surpassing even the activity of the cobalt drier. Adding more than one equivalent does not seem to enhance the rate any further, however, see Table 3.1.

To investigate the influence of bipyridine in more detail, the complex [Mn^{II}(acac)$_2$(bpy)] was synthesised separately[4] (see also Chapter 6) and was tested for its autoxidation activity. A rather large induction time is observed when this manganese(II) compound is used in combination with purified EL (Table 3.1). Initiation does not occur with manganese(II) complexes in the absence of peroxides, since manganese(II) is not able to oxidize the substrate under these reaction conditions. Thus an induction time of over 400 minutes is observed in which either the substrate or the complex is slowly air-oxidised, after which the catalytic radical autoxidation can start. To check whether the induction time indeed results from the absence of peroxides, the oxidation experiment

was also performed with unpurified EL. Then indeed no induction time is observed and the oxidation reaction starts immediately with a rate of $4*10^{-3}min^{-1}$, comparable to the rates observed for [Mn(acac)$_3$] with bpy added *in situ*.

3.2.2 Variation of the double bonds in EL followed by Raman spectroscopy

The variation of the double bonds in EL was followed in time using Raman spectroscopy, for the autoxidation of EL with different catalysts. Over the course of an autoxidation experiment, the non-conjugated *cis* double bonds in the pentadiene moiety in EL first become *trans, cis*-conjugated (see Chapter 1) and eventually, isolated *trans*.[5] Raman spectroscopy proved to be a very suitable technique to detect the changes in the various types of double bonds,[6-8] due to their high Raman absorbance. Conjugated (1599, 1634 cm^{-1}), non-conjugated *cis*-C=C (1655 cm^{-1}), and isolated *trans*-C=C (1670 cm^{-1}) bonds could be easily differentiated.[7]

In the absence of a catalyst, the peaks in EL due to double bonds did not change, not even over a period of 130 h.[7] In the presence of Co-EH, as illustrated in Figure 3.2a, the C=C-related peaks of EL showed significant changes within 1 h. After 1 h of oxidation, the non-conjugated *cis*-C=C peak (1655 cm^{-1}) and the *cis*-C=CH rock peak (1265 cm^{-1}) started to decrease while the conjugated-C=C (1599, 1634 cm^{-1}) peaks started to form. After a few hours of reaction, the amount of the conjugated-C=C bonds reached maximum levels. After that, both the non-conjugated *cis*-C=C and conjugated-C=C peaks of EL decreased substantially, eventually resulting in low amounts of C=C bonds (including isolated *trans*-C=C at 1670 cm^{-1} and some conjugated C=C) after 100 h.

The C=C related peaks of EL in the presence of [Mn(acac)$_3$] showed similar variations (Figure 3.2b), however, the conversion appeared to be at a much lower rate compared to that in the presence of Co-EH. For instance, after 21 h of oxidation, the intensity of the non-conjugated *cis*-C=C (1655 cm^{-1}) peak was still relatively high.

As is shown in Figure 3.2c, conjugated-C=C Raman peaks (1599, 1634 cm^{-1}) of EL already formed after 1 h when bpy was added to [Mn(acac)$_3$], while *cis*-C=C related peaks decreased. The time evolution of the double bond peaks appeared to proceed in a very similar manner compared to the Co-EH-catalysed system. Careful examinations reveal that in the early stage of oxidation (1–3 h), the intensity of conjugated peaks was slightly higher for the [Mn(acac)$_3$]/bpy system than for the Co-EH catalyst, indicating an even faster reaction in the presence of [Mn(acac)$_3$]/bpy. This is in agreement with the rate of disappearance of the 3010 cm^{-1} IR band (vide supra).

3.2.3 Oxygen uptake during EL oxidation

In Figure 3.3 the O_2 uptake results are shown for EL without any catalyst, as well as in the presence of the catalysts Co-EH, [Mn(acac)$_3$], and [Mn(acac)$_3$]/bpy. In the absence of a catalyst, virtually no dioxygen was taken up by EL for the entire duration of the experiment (100 h). In the presence of Co-EH, a significant amount of O_2 is taken up by the system, up to about 2.35 mol/mol EL after 100 h. A noticeably smaller amount of O_2 (1.55 mol/mol EL) was consumed when [Mn(acac)$_3$] was used as a catalyst. The uptake of O_2 by EL was enhanced when bpy was combined with [Mn(acac)$_3$]: not only a

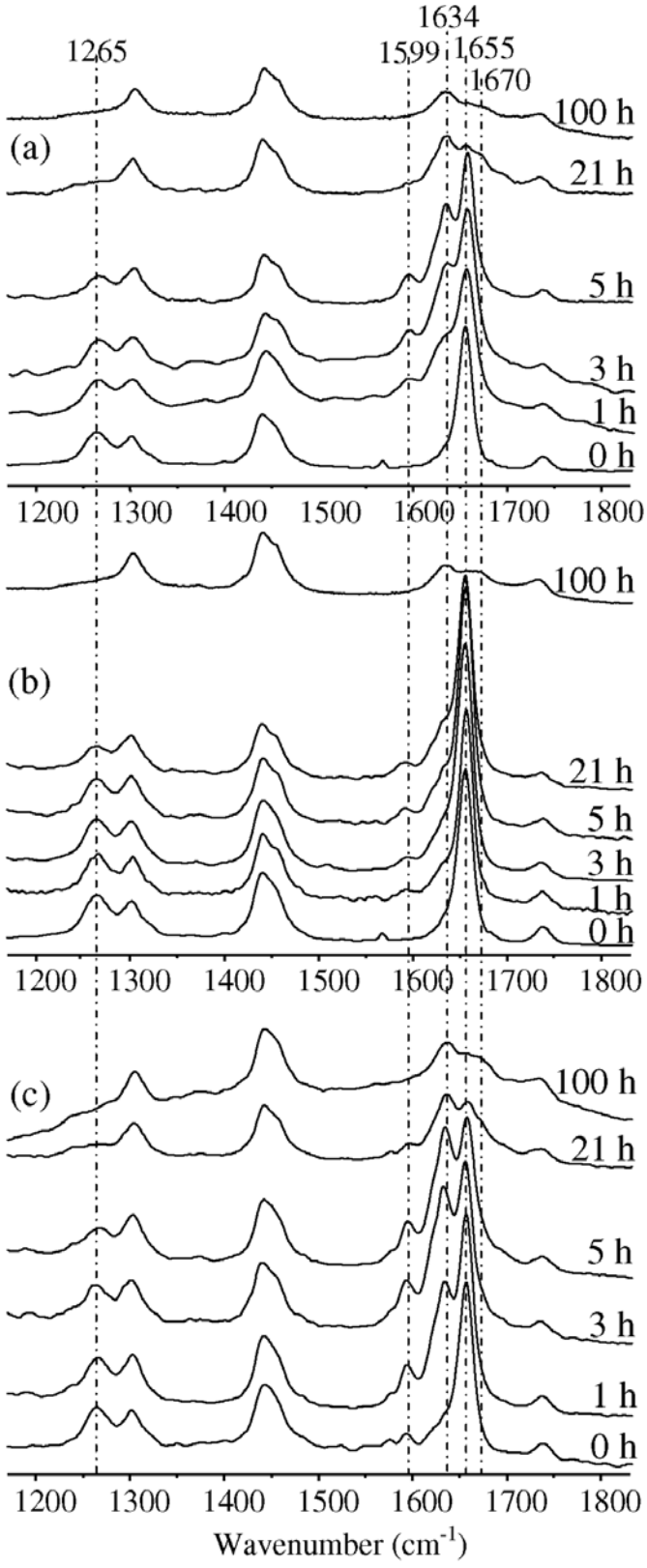

Figure 3.2: Raman spectra (1200-1800 cm^{-1}) recorded after increasing oxidation times of EL in the presence of (a) Co(II)-2-ethylhexanoate, (b) [Mn(acac)$_3$], and (c) [Mn(acac)$_3$]/bpy.

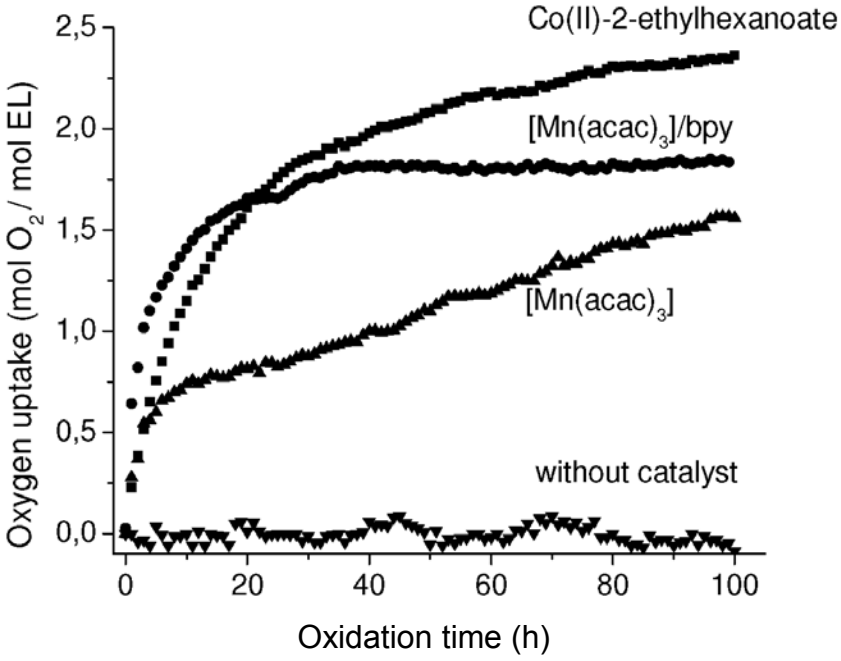

Figure 3.3: O_2 uptake during the autoxidation of EL in the presence of various catalysts, as measured using a fiber-optic oxygen meter.

larger amount of dioxygen (1.85 mol/mol EL) was taken up, also the rate of O_2 uptake was considerably higher. Interestingly, a plateau level for the O_2 consumption was reached after about 35 h when [Mn(acac)$_3$]/bpy was used, whereas in the case of [Mn(acac)$_3$] and Co-EH no plateau has yet been reached even after 100-h oxidation.

3.2.4 The time-evolution of peroxides in EL oxidation

The concentration of peroxides was monitored in time for the autoxidation of EL in the presence of the various catalysts, and the results are shown in Figure 3.4. The peroxide value for the unreacted EL, straight from the bottle received from the supplier, was determined to be 4 mmol/mol EL. In the presence of Co-EH a peroxide concentration was reached of about 50 mmol/mol in 5 h. As the oxidation of EL proceeded, the amount of peroxides increased continuously and a maximum value of 170 mmol/mol was reached in about 30 h. Then, the peroxide value decreased rapidly to a level of approximately 40 mmol/mol. These observations are in accordance with EL-autoxidation studies reported by Mallegol et al.[9, 10]

In the presence of [Mn(acac)$_3$], a much higher concentration of peroxides (240 mmol/mol) was reached after a much longer reaction time of 100 h and the rate-of-decrease of the peroxide value after attaining the maximum value was much less than for the oxidation with Co-EH. Even after 300 h a significant amount of peroxides of 130 mmol/mol still remained.

When bpy is added to [Mn(acac)$_3$], a totally different observation can be made (Figure 3.4). The concentration of peroxides was, at all times, much lower than was observed for the other two cases: a maximum value was reached of about 45 mmol/mol in

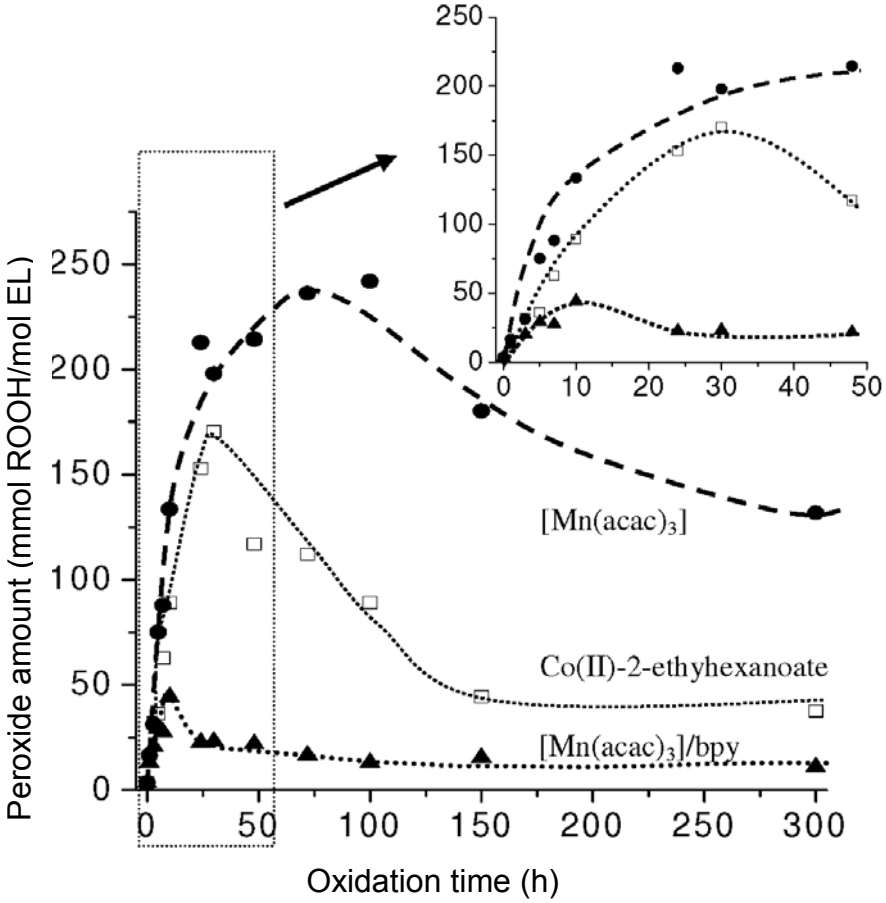

Figure 3.4: The evolution of peroxide amounts during the oxidation of EL in the presence of various catalysts. Lines are added to aid the eye

just 10 h of reaction time. The amount of peroxides then decreased to a very low level of 10 mmol/mol over the course of the experiment (up to 300 h).

3.2.5 Formation of volatile byproducts during EL oxidation

The characteristic odour of air drying alkyd paints is due to the formation of volatile aldehydes, typically hexanal and pentanal. These aldehydes are formed through β-scission reactions of alkoxy radicals,[16] as is schematically illustrated in Figure 3.6. The amount of hexanal and pentanal formed during the oxidation of EL in the presence of different catalysts was quantified by head-space GC-MS, as shown in Figure 3.5. In the reaction catalysed by Co-EH, the amount of hexanal and pentanal increased steadily over the course of the reaction (105 h), reaching levels of 16.6 and 0.4 mmol/mol EL, respectively. During the first 50 h of the oxidation with the [Mn(acac)$_3$]/bpy system much more hexanal was generated than when Co-EH was used (Figure 3.6a). However, after 100 h the hexanal levels for both catalysts were found to be at a similar level. The amount of pentanal that was generated with the [Mn(acac)$_3$]/bpy catalyst was significantly higher. In the oxidation with only [Mn(acac)$_3$] as a catalyst, lower amounts of both hexanal and pentanal were formed compared to the reactions with Co-EH or [Mn(acac)$_3$]/bpy.

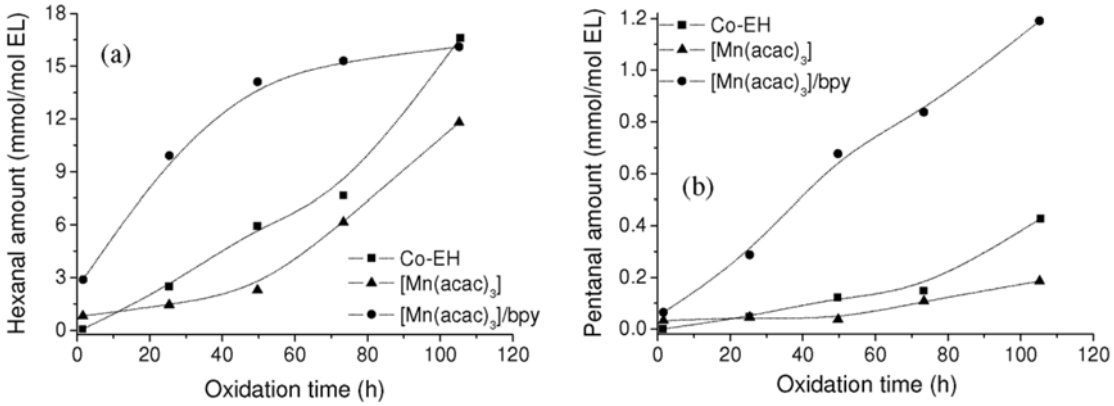

Figure 3.5: The formation of volatile byproducts (a) hexanal and (b) pentanal during the oxidation of EL in the presence of different catalysts.

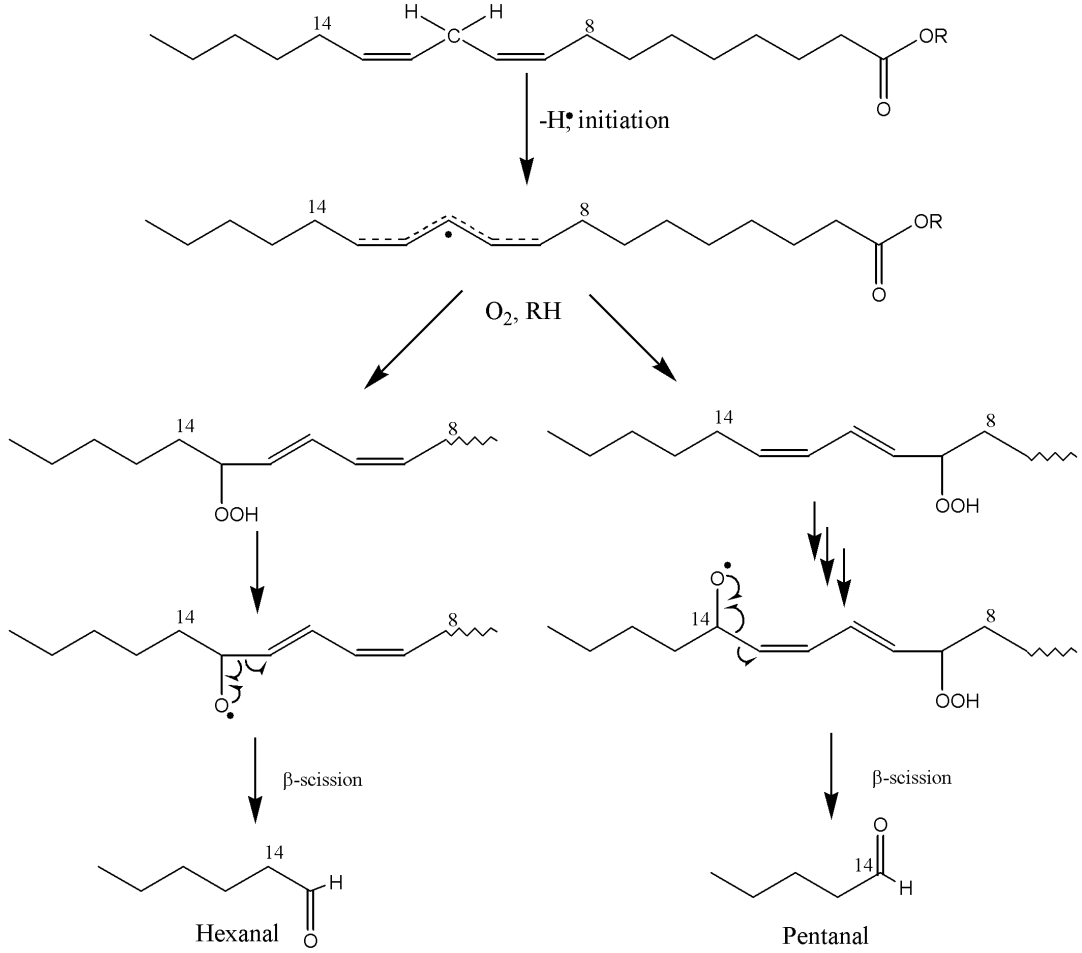

Figure 3.6: Schematic illustration of the formation of the autoxidation by-products hexanal and pentanal *via* β-scission.[16]

3.2.6 Oligomerisation during EL oxidation

The oxidation reactions of EL generally lead to the formation of oligomers, which is pivotal for the drying and hardening of real alkyd coatings. In Figure 3.7 the SEC chromatograms are shown of EL after various periods of oxidation catalysed by Co-EH,

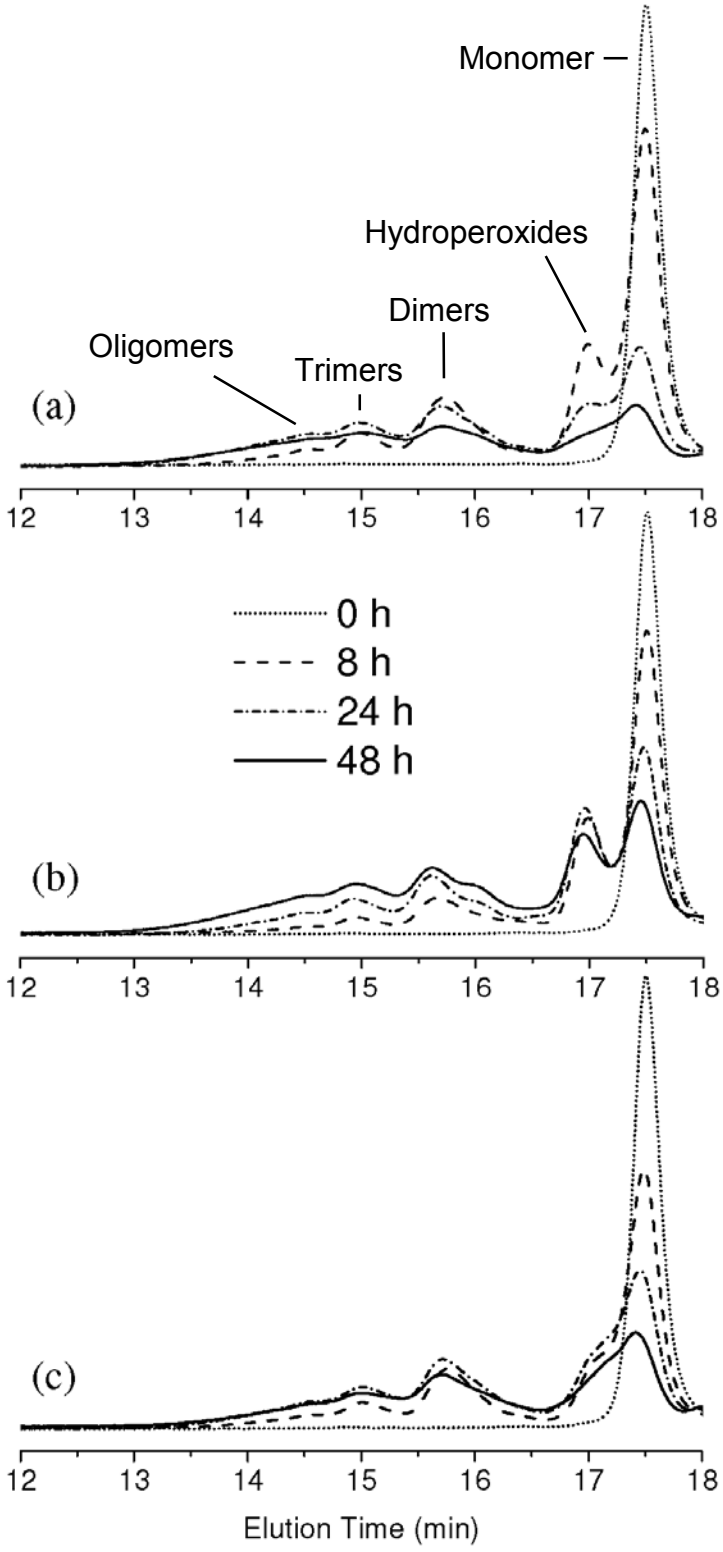

Figure 3.7: Size exclusion chromatograms of EL after different periods of oxidation in the presence of various catalysts: (a) Co(II)-2-ethylhexanoate, (b) [Mn(acac)$_3$], and (c) [Mn(acac)$_3$]/bpy.

[Mn(acac)$_3$], and [Mn(acac)$_3$]/bpy. After oxidation of EL for 8 h catalysed by Co-EH, dimers (the peak at an elution time of 15.7 min), trimers (at 15 min) and higher oligomers (13-14.5 min) could be readily observed (Figure 3.7a). As the oxidation proceeded for 24 h, more trimers and higher oligomers were formed as the dimer peak slightly decreased.[11] After 48 h, both the dimer and trimer peaks have decreased relative to their levels after 24 h, due to the formation of higher oligomers and due to oxidative degradation of the fatty acid chains *via* β-scission reactions, as was shown in the previous section. The EL peak did not disappear completely even after 48 h, which is most likely due to the presence of about 8% of non-reactive saturated esters and the presence of 19% of the less reactive ethyl oleate [11, 12] in the technical grade EL. The peak appearing at 17 min is due to EL hydroperoxides [13-15] and other oxygen-containing EL derivatives (for example, epoxide species).[15] The amount of hydroperoxides first increased and then significantly decreased over the course of the reaction (Figure 3.7a), in agreement with the results obtained for the peroxide value determination (Section 3.2.4).

In the oxidation of EL with [Mn(acac)$_3$], the same observations can be made after 8 h as for the oxidation with Co-EH, dimers and trimers are formed although to a lesser extent than for the Co-EH catalysed reaction. In contrast to the oxidation with Co-EH, however, the amount of (higher) oligomers only *increased* with prolonged reaction times, indicating little degradation of the oligomerised polymer network. This observation is in agreement with the head-space GC-MS results (see previous Section), which showed less hexanal and pentanal formation for [Mn(acac)$_3$] in comparison with the other catalysts. The peak due to hydroperoxides remains significant for the entire duration of the experiment (48 h), again in agreement with the results obtained for the peroxide value determination for the oxidation with [Mn(acac)$_3$]. The peak due to the EL-monomer also remains considerable, which is in perfect agreement with the difference in the EL oxidation rates, as were found for Co-EH and [Mn(acac)$_3$] using FT-IR.

In the oligomerisation of EL with [Mn(acac)$_3$]/bpy, the same trends in the formation of dimer, trimer and higher oligomers can be seen as for the oxidation with Co-EH (Figure 3.7c). Also for this catalyst a decrease in the dimer and trimer peaks is observed over time, which can in part be attributed to degradation of the polymer network, as is clear from the GC-MS results discussed in the previous Section. The peroxide peak is rather low in intensity at all times, in accordance with the observations made in the peroxide value determination (Figure 3.4).

3.2.7 Cyclic voltammetry

In order to compare the oxidising power of the complex [Mn(acac)$_3$] with and without bipyridine, cyclic voltammetry has been used.[17] The cyclic voltammograms of [Mn(acac)$_3$] and [Mn(acac)$_2$(bpy)] are shown in Figure 3.8. The Mn(II)/Mn(III) couple (peaks 1/1' and a/a' in Figure 3.8) shifts towards more positive potential for [Mn(acac)$_2$(bpy)] as compared to [Mn(acac)$_3$]. The voltammograms of [Mn(acac)$_2$(bpy)] obtained at different scan rates show that the relative intensity of peak a' increases with increasing scan rate, as is shown in Figure 3.9. This indicates that the species [Mn^{III}(acac)$_2$(bpy)]$^+$ is unstable under these conditions and thus it is not unlikely that the more stable [Mn(acac)$_3$] complex is formed. Peak b then results from the oxidation of [Mn(acac)$_3$] and peak b' from the reduction of [Mn^{IV}(acac)$_3$]$^+$. Indeed the fact that the Mn(III)/(IV) transitions in the voltammograms (peaks 2,2' and b/b') occur nearly at the

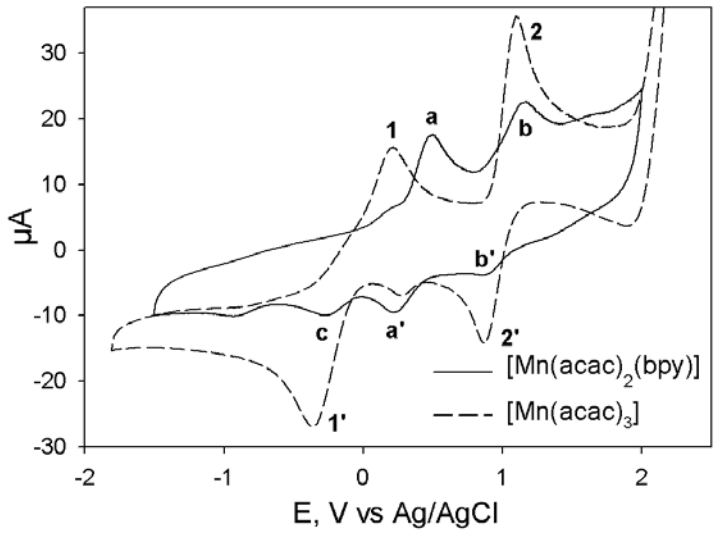

Figure 3.8: Cyclic voltammograms of [Mn(acac)$_3$] and [Mn(acac)$_2$(bpy)] in CH_3CN, [^{n}Bu$_4$N](PF$_6$) as electrolyte, scan rate 200mV/s Selected potentials:
1/1' 0.222/-0.373 V; a/a' 0.50/0.203 V; 2/2' 1.111/0.862 V; b/b' 1.165/0.891 V; c –0.28 V.

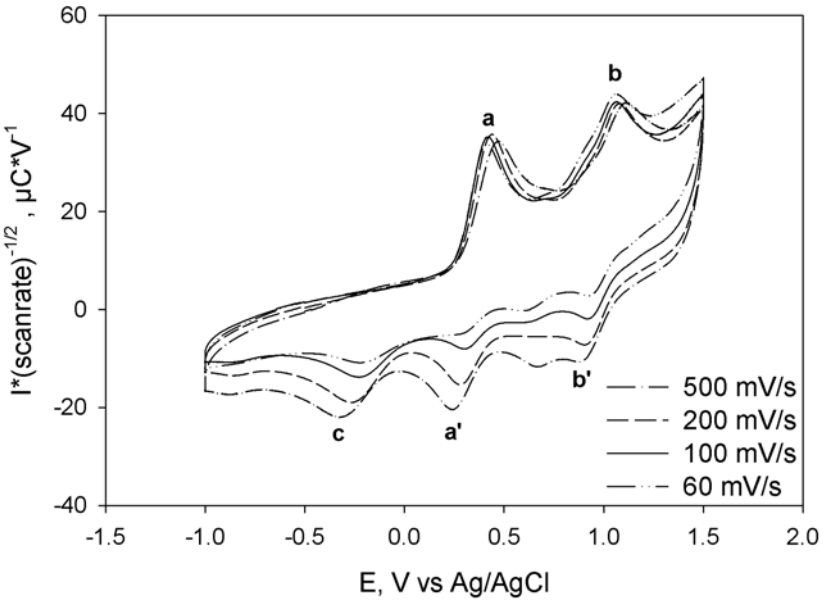

Figure 3.9: CV's of [Mn(acac)$_2$(bpy)], recorded at different scan rates.

same potentials, suggest also that they must both arise from the same species, i.e. [Mn(acac)$_3$]. Peak c most probably results from the reduction of [Mn^{III}(acac)$_3$] to [Mn^{II}(acac)$_3$]$^-$, as can be concluded by comparison with peak 1'. The reduced complex [Mn^{II}(acac)$_3$]$^-$ reacts with bpy in solution to form the more stable complex [Mn^{II}(acac)$_2$(bpy)], which is supported by the absence of a (re)oxidation peak for [Mn^{II}(acac)$_3$]$^-$. The cyclic voltammogram of an in situ mixture of [Mn(acac)$_3$] with bpy was found to be nearly identical to that of [Mn(acac)$_2$(bpy)], confirming the instability of the complexes and the occurrence of rapid equilibrium reactions.

3.2.8 Experiments in real alkyd paint

The complex [Mn(acac)$_3$] was also tested as a drier in a real alkyd paint formulation, both in the absence and presence of bpy. The drying time of the paint was determined using two methods common in the paint industry: using the "thumb-test" and by making use of a Braive recorder.[18, 19] The basic principle behind a Braive recorder is that a needle is dragged over a wet film at a constant speed. The kind of trace the needle makes in the film determines in which stage of drying the film is. For a Braive drying recorder these stages are defined as: stage a: the paint is wet and flows together, the end of this stage is called the "open time"; stage b: a scratchy line is visible, the paint begins to polymerise, the end of this stage is the "dust-free time"; and stage c: the needle traces a straight line in the film, the end of this phase is the "surface dry time".

In the "thumb-test" method, a thumb is pressed to the paint layer to see what kind of mark is left. The drying times for [Mn(acac)$_3$] and [Mn(acac)$_3$]/bpy and the results obtained for commercial combination cobalt and manganese driers are listed in Table 3.2.[19] From the results presented in Table 3.2, it is clear that [Mn(acac)$_3$] and [Mn(acac)$_3$]/bpy have paint-drying activities which are *considerably* better than the activities of the standard manganese paint driers, since the total drying times are halved for the new driers. The drying results compared to the drying times obtained with cobalt are comparable or even slightly better. It is also interesting to note that the drying times for [Mn(acac)$_3$] appear to be even shorter than for the [Mn(acac)$_3$]/bpy system.

Table 3.2: Drying times of real alkyd paint, using different catalysts.[a]

	Drying time by hand		Braive recorder drying time		
Drier	surface dry	through dry	stage a	stage b	stage c
Co-Ca-Sr [b]	1 h 45 min	2 h 15 min	1 h 15 min	2 h 15 min	6 h 45 min
Mn-Ca-Zr [c]	> 6 h	--	1 h 30 min	12 h 30 min	16 h
Mn-bpy [d]	3 h	> 6 h	1 h 30 min	6 h 30 min	10 h
[Mn(acac)$_3$]	2 h	2 h 30 min	1 h 15 min	2 h 15 min	4 h
[Mn(acac)$_3$] + bpy	2 h 30 min	3 h	1 h 15 min	3 h	5 h

[a]The drying time was measured in a clear varnish based on Uralac AD 152 WS-40 from DSM Resins (a medium oil alkyd resin based on soy-bean oil, 47% oil). [b]Commercial cobalt combination drier. [c]Commercial manganese combination drier. [d]Commercial manganese drier based on manganese 2-ethylhexanoate and bipyridine.

3.3 Discussion

3.3.1 Autoxidation and oligomerisation of EL by different catalysts

3.3.1.1 Radical initiation by [Mn(acac)$_3$]

Mn(III) is well known as a radical initiator, mostly in the form of [Mn(OAc)$_3$] in acetic acid, at elevated temperatures and often in the presence of radical-chain starters such as NHPI (N-hydroxy-phtalimide).[20-22] [Mn(acac)$_3$] in combination with co-catalysts such as acetic acid[23, 24] or benzyl bromide[25] is also known to act as a radical initiator in the radical polymerisation of various substrates.

The induction time in the oxidation of EL is a measure of the ability of the catalyst to initiate the autoxidation radical-chain reaction. Consequently, from the short induction times observed in the FTIR measurements it seems that [Mn(acac)$_3$] is able to initiate the

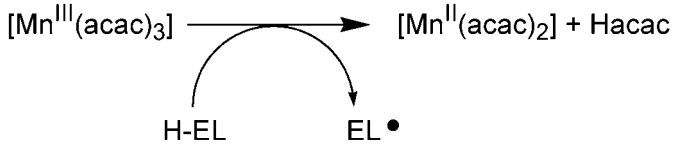

Scheme 3.1: Radical initiation by [Mn(acac)$_3$] through hydrogen atom abstraction of the activated methylene group in ethyl linoleate.

radical autoxidation of EL *directly* and at room temperature. Initiation thus occurs even in absence of any acids, halides, peroxides or other easily oxidisable radical chain starters. A tentative mechanism for the initiation reaction is depicted in Scheme 3.1. Radical initiation is proposed to occur *via* a hydrogen atom abstraction pathway, in analogy with a mechanism for the oxidation of 1,4-cyclohexadiene by tris(hexafluoroacetylacetonato)-manganese(III) as described by Bryant *et al.*[26] H-atom transfer from EL to [Mn^{III}(acac)$_3$] results in the formation of [Mn^{II}(acac)$_2$], a free acetylacetone ligand and an ethyl linoleate radical (EL$^{\bullet}$). This ethyl linoleate radical reacts immediately with dioxygen to form a peroxy radical, which can form a hydroperoxide by again abstraction of an H$^{\bullet}$ from another EL molecule.

3.3.1.2 Oxidation of EL

The Raman and FTIR results show that [Mn(acac)$_3$] catalyses the oxidation of EL at a reasonable rate, although this rate is lower than for the oxidation with Co-EH. In the Raman spectra for the [Mn(acac)$_3$]/bpy system, at t = 0 a small peak is visible that is due to conjugation (1599 cm^{-1}) of double bonds, a sure sign that the oxidation reaction has already started. The Raman spectra and the rate of oxygen uptake for the catalysts Co-EH and [Mn(acac)$_3$]/bpy clearly show that the rate of oxidation of EL is higher for the [Mn(acac)$_3$]/bpy system, a result which is in agreement with the FTIR data. From the data of the amounts of peroxide, it becomes clear that the high oxidation rate for the [Mn(acac)$_3$]/bpy system might be attributed to an extremely efficient capability of hydroperoxide decomposition.

Scheme 3.2 shows the set of radical reactions that are often proposed for hydroperoxide (ROOH) build-up in metal-catalysed autoxidation reactions (see also Chapter 1, Scheme 1.1).[27] The hydroperoxide concentration, at a given time, depends on the ratio of the rates for hydroperoxide decomposition vs hydroperoxide formation.[28] According to the reactions in Scheme 3.2, the higher the rate for reactions **4** and **5**, the lower the hydroperoxide concentration will be. It appears that the [Mn(acac)$_3$]/bpy catalyst is able to decompose ROOH almost as soon as it is formed, thus attaining a very

RH + Initiator $\rightarrow$ R$^{\bullet}$	**1**
R$^{\bullet}$ + O$_2$ $\rightarrow$ ROO$^{\bullet}$	**2**
ROO$^{\bullet}$ + RH $\rightarrow$ ROOH + R$^{\bullet}$	**3**
ROOH + M^{n+} $\rightarrow$ RO$^{\bullet}$ + OH$^-$ + M$^{(n+1)+}$	**4**
ROOH + M$^{(n+1)+}$ $\rightarrow$ ROO$^{\bullet}$ + H$^+$ + M^{n+}	**5**

Scheme 3.2: General metal-catalysed (M) autoxidation reactions, which are responsible for hydroperoxide (ROOH) build-up

Co-EH catalyst

$Co^{II} + O_2 + RH \rightleftharpoons Co^{III}OO^{\bullet} + RH \rightarrow R^{\bullet} + Co^{III}OOH$ **6**

$Co^{II} + ROOH \rightarrow RO^{\bullet} + [Co^{III}(OH^-)]$ **7**

$[Co^{III}(OH^-)] + ROOH \rightarrow Co^{II} + ROO^{\bullet} + H_2O$ **8**

$[Mn(acac)_3]$ catalyst

$[Mn^{III}(acac)_3] + ROOH \rightarrow [Mn^{II}(acac)_2(Hacac)] + ROO^{\bullet}$ **9**

$[Mn^{II}(acac)_2(Hacac)] + ROOH \rightarrow [Mn^{III}(acac)_3] + RO^{\bullet} + H_2O$ **10**

$[Mn^{III}(acac)_3] + RH \rightarrow [Mn^{II}(acac)_2(Hacac)] + R^{\bullet}$ **11**

$[Mn(acac)_3]$/bpy catalyst

$[Mn^{II}(acac)_2(Hacac)] + bpy \rightarrow [Mn^{II}(acac)_2(bpy)] + Hacac$ **12**

$[Mn^{II}(acac)_2(bpy)] + ROOH \rightarrow [Mn^{III}(acac)_2(bpy)]^+(OH^-) + RO^{\bullet}$ **13**

$[Mn^{III}(acac)_2(bpy)]^+(OH^-) + ROOH \rightarrow [Mn^{II}(acac)_2(bpy)] + ROO^{\bullet} + H_2O$ **14**

$[Mn^{III}(acac)_2(bpy)]^+(OH^-) + RH \rightarrow [Mn^{II}(acac)_2(bpy)] + R^{\bullet} + H_2O$ **15**

Scheme 3.3: Proposed sets of reactions for each of the catalyst systems.

low ROOH concentration. In Scheme 3.3, a tentative overview is given for the metal-catalysed peroxide decomposition reactions for each catalyst used in the present study.

The cobalt catalyst is mainly a robust peroxide decomposition catalyst, where the rate for reaction **7** will probably be comparable to the rate for reaction **8**. It is clear from Figure 3.4, where the ROOH concentration decreases steadily after the maximum has been reached, that the cobalt catalyst retains its decomposition activity for at least 150 h. The oxygen uptake data for the Co-EH-catalysed EL oxidation show that significant over-oxidation of EL takes place (oxygen uptake higher than 1 mol O_2/mol EL). The most common pathways for over-oxidation are: (1) through radical addition to conjugated double bond systems, generating a new carbon-centered radical which can again react with dioxygen,[29] or (2) via oxidation of the products generated by a β-scission reaction of an alkoxyl radical.

Reactions **9** and **10** in Scheme 3.3 are the proposed ROOH decomposition reactions for the catalyst $[Mn(acac)_3]$. Additionally, the direct activation of EL *via* reaction **11** also plays a role for $[Mn(acac)_3]$, as was also shown in Scheme 3.1. The most important difference for the activity of $[Mn(acac)_3]$ compared to Co-EH is the rate with which reactions **9** and especially **10** proceed (apparent from the Raman data and the rate for oxygen uptake). A lower rate for these reactions can explain the significantly higher hydroperoxide concentration that is attained through reactions **2** and **3** in Scheme 3.2. Additional hydroperoxides can be formed through reaction **11** in Scheme 3.3.

As mentioned above, the $[Mn(acac)_3]$/bpy catalyst shows a *very* high rate for the oxidation of EL. The high oxidation activity is ascribed to the *in-situ* formation of the compound $[Mn^{II}(acac)_2(bpy)]$ through the sequence of reactions **9** and **12** (or **11** and **12**). The species $[Mn^{II}(acac)_2(bpy)]$ has most probably a very high rate for reaction **13**,

forming species $[Mn^{III}(acac)_2(bpy)]^+$. The cyclic voltammetry measurements have shown that this complex has a reduction wave at 0.203 V (vs Ag/AgCl in CH_3CN). This makes the species $[Mn^{III}(acac)_2(bpy)]^+$ a much more potent oxidising agent than for example $[Mn^{III}(acac)_3]$, which has the corresponding reduction wave at –0.373V (vs Ag/AgCl in CH_3CN). The reduction of Mn(III) is always the slower reaction in the Haber-Weiss reactions,[20] and addition of bpy thus effectively "de-bottlenecks" the autoxidation reaction, by speeding up the slower step. Reactions **13, 14** and **15** in Scheme 3.3 will thus proceed at a much higher rate than reactions **9**, **10** and **11**. The extremely high rate of dioxygen uptake, coupled to the very low levels of detected hydroperoxides may be explained by the assumption that the oxidation will most likely be dominated by reactions **13** and **15**, once the species $[Mn^{II}(acac)_2(bpy)]$ is formed. The alkoxy radicals that are formed in reaction **13** have a high tendency to undergo β-scission, thus forming hexanal and pentanal (see Figure 3.6). Formation of alkoxy radicals disrupts the radical chain of reactions **2** and **3** (Scheme 3.2), and consequently the build-up of a high ROOH concentration. An explanation for the complete stop of the uptake of oxygen once all hydroperoxides are decomposed (compare Figs 3.3 and 3.4 after a reaction time of 35 h) could be that the complex $[Mn^{III}(acac)_2(bpy)]^+$ can only rapidly abstract a doubly allylic hydrogen atom. Once each molecule of EL has reacted with at least one molecule of dioxygen, no doubly allylic hydrogen atoms and hydroperoxides are available anymore (since hydroperoxides are rapidly decomposed) and reactions **13**, **14** and **15** will stop.

3.3.1.3 Oligomerisation of EL

A major difference between the SEC results for Co-EH and [Mn(acac)$_3$] is the amount of oligomers that are formed over a period of 48 h. The levels of dimer, trimer and higher oligomers are clearly higher for the [Mn(acac)$_3$] catalyst. This observation can be explained by the high ROOH level that is generated through the cycle of reactions **2**, **3** and reaction **11**: each hydroperoxide that is formed results in the formation of a set of conjugated double bonds, see for example the upper part of Figure 3.6. A high ROOH concentration thus implies a high concentration of conjugated double bonds which are especially prone to radical addition reactions, due to the possibility of forming a relatively stable allylic radical.[29] Consequently, each time an alkoxy or especially a peroxo radical species is formed through decomposition of a hydroperoxide, a probable reaction pathway for the radical is to react with a conjugated double bond to form a higher oligomer. Another reason for the lower level of oligomerisation as observed for Co-EH is degradation of the polymer network that is formed. The head-space GC-MS data for the Co-EH-catalysed EL oxidation reaction shows that constant hexanal and pentanal formation takes place, a sure sign for β-scission reactions. For [Mn(acac)$_3$], the amounts of hexanal and pentanal that are formed (Fig. 3.5a,b) are lower, but the same trend is followed as observed for the autoxidation of EL catalysed by Co-EH. This observation supports the assumption that a lower rate for the ROOH decomposition reactions is probably the most prominent difference between the oxidation mechanisms by which [Mn(acac)$_3$] and Co-EH function.

The SEC chromatogram for the oxidation of EL catalysed by [Mn(acac)$_3$]/bpy is similar to that for the Co-EH catalysed EL oxidation, except for the low intensity of the hydroperoxide-peak (in agreement with the results for the hydroperoxide determination, Fig 3.4). As discussed in the previous section, the [Mn(acac)$_3$]/bpy catalyst will probably

predominantly operate through reactions **13** and **15** and thus generate a higher level of alkoxy radicals relative to the other catalysts. The high amounts of hexanal and pentanal that are formed (Fig. 3.5a,b) as compared to Co-EH and [Mn(acac)$_3$] is in agreement with this assumption. A system which predominantly generates alkoxy radicals will have a lower extent of oligomerisation, since these radicals generally have more pathways to form other products of low molecular weights.[16]

3.3.2 The best paint drier

The cobalt(II) 2-ethylhexanoate catalyst is the most widely used oxidative drier for alkyd paints. Judging *only* by the oxidation rate of the alkyd model compound EL, it is tempting to say that the manganese catalyst system [Mn(acac)$_3$]/bpy would be an ideal replacement for cobalt as a drier. The results pertaining to the formation of higher oligomers show, however, that the slower catalyst [Mn(acac)$_3$] yields a much higher extent of oligomerisation. This observation is supported by the drying results in actual alkyd paint formulations,[19] where the catalyst [Mn(acac)$_3$] shows slightly better drying than the system [Mn(acac)$_3$]/bpy. In real alkyd systems, cobalt is never used as the only drier: so-called "secondary" driers are added, sometimes even to *retard* the activity of the cobalt drier.[30] The lower performance for [Mn(acac)$_3$]/bpy in real alkyd paint (see Table 3.2) might indeed be attributed to the fact that it is *too* active: the autoxidation reactions yield predominantly alkoxy radicals, which results in less oligomerisation. Thus although the [Mn(acac)$_3$] catalyst shows a lower rate of oxidation, as a paint drier it is the better candidate to replace the cobalt catalyst.

3.4 Conclusions

The compound [Mn(acac)$_3$] is an efficient catalyst for the oxidation and the oligomerisation of EL, which is proposed to proceed not only *via* hydroperoxide decomposition, but also through substrate activation. [Mn(acac)$_3$] was also found to function as a very good drying catalyst in a real alkyd system, better than conventional manganese driers and comparable to, or even better than a cobalt combination drier. The system [Mn(acac)$_3$] with bpy added has a very high activity for the oxidation of EL. *In-situ* formation of the species [Mn^{II}(acac)$_2$(bpy)] and [Mn^{III}(acac)$_2$(bpy)]$^+$ and the high reactivities of these two species with ROOH and EL, respectively, were proposed as an explanation for the observed high oxidation rate. In the oxidation of EL by the [Mn(acac)$_3$]/bpy catalyst less oligomerisation and a higher amount of volatile products is observed, probably due to the generation of predominantly alkoxy radicals in hydroperoxide decomposition. In real alkyd systems, adding bpy to [Mn(acac)$_3$] is therefore not advantageous, as is also evident from the longer drying times that have been observed for [Mn(acac)$_3$]/bpy in a real alkyd system as compared to the drying times for [Mn(acac)$_3$].

3.5 Experimental

3.5.1 Materials

Technical grade ethyl linoleate (EL), containing 73% EL, 19% ethyl oleate, 6% ethyl palmitate, and 2% ethyl stearate as determined by GC-MS, and Mn(III) acetylacetonate, [Mn(acac)$_3$], were obtained from Fluka. 2,2'-bipyridine (bpy) and Co(II) 2-ethylhexanoate (Co-EH, 65% w/w solution in white spirit) were obtained from Sigma-Aldrich. Mn 2-ethylhexanoate (Mn Nuodex) was received as a gift from Servo. Chemicals were used as received unless stated otherwise.

3.5.2. Instrumentation and procedures

3.5.2.1. Raman & FTIR spectroscopy

The autoxidation of EL was followed by FTIR spectroscopy according to the method described in Chapter 2. Raman spectroscopy was performed at the technical university of Eindhoven (TUE), using a Dilor-Jobin Yvon-Horiba confocal dispersive Raman spectrometer (633 nm excitation wavelength, 1000 μm pinhole, and 8 mW laser intensity) with an Olympus MX40 microscope. EL containing 0.07 wt% of different catalysts was deposited (~ 200 μm) onto glass slides for *in-situ* Raman analysis. In the experiments involving bpy, 3 molar equivalents of bpy were added relative to [Mn(acac)$_3$].

3.5.2.2 Oxygen uptake (performed at TUE)

A Fibox fiber-optic oxygen meter (Precision Sensing GmbH) was used to measure the oxygen uptake of EL in the presence of various catalysts. The dioxygen meter consists of a dioxygen sensor probe (PSt3). The tip of the probe is coated with a Pt(II) indicator dye embedded in a silicone matrix, which is connected to a LED (excitation wavelength: 505 nm) through a fiber optic cable, a photomultiplier detector (PMT). A PT 100 type temperature sensor is used for temperature compensation (details can be found at http://www.presens.de).

For the oxygen uptake measurement at room temperature (~ 21 °C), 4 g of EL, premixed with a catalyst (0.07 wt%), was placed into a 6-L sealed container filled with air at a normal atmospheric pressure, equipped with oxygen and temperature sensors inside. When [Mn(acac)$_3$] was used, it was first dissolved in a small amount of toluene. The consumed oxygen concentration was expressed as mol oxygen per mol of EL.

3.5.2.3 Peroxide value determination (performed at TUE)

An American Oil Chemists' Society (AOCS)-approved method for determining peroxide value (PV) was used with some modifications.[31] EL (40 g) was mixed with a catalyst (0.07 wt%) and placed in a Petri dish (~ 20 cm radius) for oxidation at room temperature (21 ^{o}C, 50% RH). About 2 g of EL was withdrawn from Petri dishes for PV measurements. Samples were dissolved in 30 mL of a mixture of glacial acetic acid/chloroform (3:2 v/v). 0.5 mL of saturated potassium iodide solution (in excess) was added followed by the addition of 30 mL of deionised water and 0.5 mL of starch dispersion (5 g/L). The solution was titrated with sodium thiosulfate solution (0.02 N), until the yellow/brown colour fully disappeared. The results were corrected with a blank

sample that did not contain EL. Duplicate measurements were performed for each sample and average values were taken. The accuracy of the method was checked by the titration of H_2O_2 and cumene hydroperoxide, and it was found that the difference between experimental values and theoretical values was less than 2%.

3.5.2.4. Size exclusion chromatography (performed at TUE)

The oligomerisation of EL was followed by size exclusion chromatography (SEC) on a Waters GPC instrument equipped with a Waters model 510 pump and a model 410 differential refractometer (40 °C); THF was used as the eluent. Samples were withdrawn from Petri dishes and dissolved in THF (1 mg/mL). The method described here differs from the general method described in Chapter 2.

3.5.2.5. Head-space gas chromatography – GC-MS (performed at TUE)

EL (1 g) was first mixed with different catalysts (0.07 wt%). An aliquot of 10 mg was placed in a 20-mL head-space vial for each measurement, followed by the addition of 1 μL of cyclohexane solution (0.37 M in xylene) as an internal standard. Vials were then sealed with silicon rubber Teflon® caps using a crimper. EL was oxidized in the sealed vials in the presence of catalysts. Several vials were prepared and, at different time intervals, volatile byproducts were determined on a Thermoquest CE 2000 series trace GC-MS equipped with static head-space autosampler (HS 2000 model). Trace GC was equipped with a capillary column (based on silica, length 60 m × 0.25 mm, 0.25 μm thickness, Alltech). Helium was used as a carrier gas, and ionisation mode of the trace MS was electron impact (EI+). All of the intricate operations of establishing an equilibrium in static head-space analysis was performed by the HS 2000 robotic autosampler through a local controller using Windows®-based software. After reaching equilibration, the heated gas-tight head-space syringe (45 °C) was moved over the incubator by a turret and a sample was withdrawn. The turret was turned to the position over the inlet, and the injection was made. The syringe was then automatically cleaned with a purged carrier gas (He). For the programmable temperature vaporisation (PTV) injector method, the base temperature was 43 °C with a split flow of 50 mL/min. The transfer temperature to the column was 325 °C. The GC column was programmed with an initial hold of 4 min at 45 °C and then the temperature was raised to 330 °C at a rate of 10 °C/min. Peak areas for the volatiles (e.g. hexanal, pentanal) were integrated and normalised with the peak area of cyclohexane using characteristic mass ranges. The amounts of hexanal and pentanal formed during the oxidation of EL were calculated by using pure compounds of hexanal, pentanal, and cyclohexane as references. The typical experimental error for the GC-MS analysis was found to be 6%.

3.5.2.6 Cyclic voltammetry

The typical concentration of the metal complex was 12 μM in CH_3CN, electrolyte $[^nBu_4N]PF_6$, 1.2 mM. Platinum work and counter electrodes were used with a Ag/AgCl reference electrode. The working electrode was polished before each set of measurements. The starting potentials were -0.5V for $[Mn(acac)_2(bpy)]$ and –0.75V for $[Mn(acac)_3]$. The first vertex potential was +1.5V for $[Mn(acac)_2(bpy)]$ and +2.0V for $[Mn(acac)_3]$.

3.5.2.7 Drying of alkyd paint (performed at Elementis specialties, formerly Sasol Servo)

All experiments and measurements were performed at room temperature. The drying time was determined by a Braive drying recorder (wet film thickness: 76 μm; ASTM D5895-96). After the application of the film on a glass strip (30.5 × 2.5 cm) a vertical blunt needle is positioned into the freshly applied film by a 5 g load and then dragged through the drying paint in a direction parallel to the length of the coat. The three stages in the Braive recorder experiment are described as stage a: the paint flows together (leveling), *i.e.* the paint is wet; stage b: a line is visible, the paint begins to polymerize; stage c: this is the so-called "surface dry time", the paint film is no longer displaced by the needle. The drying was further established by hand according to ASTM D1640 (wet film thickness 60 μm). The through drying state was determined using a "mechanical thumb" device.

References

[1] J. H. Bieleman, in *Additives for Coatings* (Ed.: J. H. Bieleman), Wiley/VCH, Weinheim, **2000**, pp. 202.
[2] D. Lison, M. De Boeck, V. Verougstraete, M. Kirsch-Volders, *Occup. Environ. Med.* **2001**, *58*, 619.
[3] J. R. Bucher, J. R. Hailey, J. R. Roycroft, J. K. Haseman, R. C. Sills, S. L. Grumbein, P. W. Mellick, B. J. Chou, *Toxicol. Sci.* **1999**, *49*, 56.
[4] P. O. Dunstan, *Thermochim. Acta* **2000**, *356*, 19.
[5] J. Mallegol, J. L. Gardette, J. Lemaire, *J. Am. Oil Chem. Soc.* **1999**, *76*, 967.
[6] G. Ellis, M. Claybourn, S. E. Richards, *Spectroc. Acta Pt. A-Molec. Biomolec. Spectr.* **1990**, *46*, 227.
[7] Z. O. Oyman, W. Ming, R. van der Linde, *Prog. Org. Coat.* **2003**, *48*, 80.
[8] Z. O. Oyman, W. Ming, R. van der Linde, *Polymer* **2004**, *45*, 7431.
[9] J. Mallegol, J. Lemaire, J. L. Gardette, *Prog. Org. Coat.* **2000**, *39*, 107.
[10] J. Mallegol, L. Gonon, S. Commereuc, V. Verney, *Prog. Org. Coat.* **2001**, *41*, 171.
[11] W. J. Muizebelt, J. C. Hubert, R. A. M. Venderbosch, *Prog. Org. Coat.* **1994**, *24*, 263.
[12] E. N. Frankel, *J. Am. Oil Chem. Soc.* **1984**, *61*, 1908.
[13] S. T. Warzeska, M. Zonneveld, R. van Gorkum, W. J. Muizebelt, E. Bouwman, J. Reedijk, *Prog. Org. Coat.* **2002**, *44*, 243.
[14] S. Tanase, E. Bouwman, J. Reedijk, *Appl. Catal. A-Gen.* **2004**, *259*, 101.
[15] W. J. Muizebelt, J. J. Donkerbroek, M. W. F. Nielen, J. B. Hussem, M. E. F. Biemond, R. P. Klaasen, K. H. Zabel, *J. Coat. Tech.* **1998**, *70*, 83.
[16] J. C. Hubert, R. A. M. Venderbosch, W. J. Muizebelt, R. P. Klaasen, K. H. Zabel, *Prog. Org. Coat.* **1997**, *31*, 331.
[17] R. van Gorkum, E. Bouwman, J. Reedijk, *Inorg. Chem.* **2004**, *43*, 2456.
[18] M. Ali, W. R. McWhinnie, *Applied Organometallic Chemistry* **1993**, *7*, 137.
[19] R. van Gorkum, E. Bouwman, J. Reedijk, *patent EP1382648*, **2004**
[20] R. A. Sheldon, J. K. Kochi, in *Advances in Catalysis, Vol. 25* (Eds.: D. D. Eley, H. Pines, P. B. Weisz), Academic Press, New York, **1976**, pp. 274.
[21] B. B. Snider, *Chem. Rev.* **1996**, *96*, 339.
[22] Y. Ishii, S. Sakaguchi, *Catal. Survey Japan* **1999**, *3*, 27.
[23] N. A. Lavrov, *Russ. J. Appl. Chem.* **1994**, *67*, 1358.
[24] N. A. Lavrov, *Russ. J. Appl. Chem.* **1995**, *68*, 922.
[25] K. Endo, A. Yachi, *Polym. Bull.* **2001**, *46*, 363.
[26] J. R. Bryant, J. E. Taves, J. M. Mayer, *Inorg. Chem.* **2002**, *41*, 2769.
[27] E. N. Frankel, *Lipid oxidation*, The oily press LTD, Dundee, Scotland, **1998**.
[28] L. Reich, S. Stivala, *Autoxidation of Hydrocarbons and Polyolefins*, Marcel Dekker, Inc., New York, **1969**.
[29] W. J. Muizebelt, M. W. F. Nielen, *J. Mass Spec.* **1996**, *31*, 545.
[30] R. G. Middlemiss, D. J. Olszanski, *Am. Paint Coat. J.* **1993**, *78*, 35.
[31] American Oil Chemists' Society, method *cd 8B-53* **1990**.